



LAWRENCE
LIVERMORE
NATIONAL
LABORATORY

A Numerical Investigation into the Anomalous Slight NO_x Increase when Burning Biodiesel: A New (Old) Theory

G. A. Ban-Weiss, J. Y. Chen, B. A. Buchholz, R. W. Dibble

February 1, 2007

Fuel Processing Technology

Disclaimer

This document was prepared as an account of work sponsored by an agency of the United States Government. Neither the United States Government nor the University of California nor any of their employees, makes any warranty, express or implied, or assumes any legal liability or responsibility for the accuracy, completeness, or usefulness of any information, apparatus, product, or process disclosed, or represents that its use would not infringe privately owned rights. Reference herein to any specific commercial product, process, or service by trade name, trademark, manufacturer, or otherwise, does not necessarily constitute or imply its endorsement, recommendation, or favoring by the United States Government or the University of California. The views and opinions of authors expressed herein do not necessarily state or reflect those of the United States Government or the University of California, and shall not be used for advertising or product endorsement purposes.

**A NUMERICAL INVESTIGATION INTO THE ANOMALOUS SLIGHT NO_x INCREASE WHEN BURNING
BIODIESEL; A NEW (OLD) THEORY**

CORRESPONDING AUTHOR TO WHOM PROOFS SHOULD BE SENT:

George A Ban-Weiss
50B Hesse Hall
University of California, Berkeley
Berkeley, CA 94720
Work +1 510 642 9158
Fax +1 510 642 1850
georgebw@me.berkeley.edu (preferred method of contact)

A Numerical Investigation into the Anomalous Slight NO_x Increase When Burning Biodiesel; A New (Old) Theory

George A. Ban-Weiss ^{a,*}, J.Y. Chen ^a, Bruce A. Buchholz ^b, Robert W. Dibble ^a

^aCombustion Analysis Laboratory, 50B Hesse Hall, University of California, Berkeley
Berkeley, CA 94720

^bCenter for Accelerator Mass Spectrometry, Lawrence Livermore National Laboratory,
Livermore, CA 94551

Abstract

Biodiesel is a notable alternative to petroleum derived diesel fuel because it comes from natural domestic sources and thus reduces dependence on diminishing petroleum fuel from foreign sources, it likely lowers lifecycle greenhouse gas emissions, and it lowers an engine's emission of most pollutants as compared to petroleum derived diesel. However, the use of biodiesel often slightly increases a diesel engine's emission of smog forming nitrogen oxides (NO_x) relative to petroleum diesel. In this paper, previously proposed theories for this slight NO_x increase are reviewed, including theories based on biodiesel's cetane number, which leads to differing amounts of charge preheating, and theories based on the fuel's bulk modulus, which affects injection timing. This paper proposes an additional theory for the slight NO_x increase of biodiesel. Biodiesel typically contains more double bonded molecules than petroleum derived diesel. These double bonded molecules have a slightly higher adiabatic flame temperature, which leads to the increase in NO_x production for biodiesel. Our theory was verified using numerical simulations to show a NO_x increase, due to the double bonded molecules, that is consistent with observation. Further, the details of these numerical simulations show that NO_x is predominantly due to the Zeldovich mechanism.

Keywords: Biodiesel; Diesel; Emissions; NO_x; Increase; Double bond

1.0 Introduction

Diesel engines are more efficient than spark-ignited (SI) engines, and thus emit less carbon dioxide (CO₂) per kW-hr. Diesels also generally emit less hydrocarbons (HC) and carbon monoxide (CO) than SI engines. However, oxides of nitrogen (NO_x) and particulate matter (PM) emissions have been historically much higher in diesel engines. For example, although heavy-duty diesel trucks account for only 1% of the on-road fleet, 3% of the miles traveled, and 12% of on-road fuel use [1], they are responsible for half or more of the on-road NO_x and PM emissions in California [2]. Imminent diesel engine regulations for NO_x and PM in the United States will result in a convergence of diesel and gasoline engine tail pipe emissions. It will be interesting to observe how the market share for the diesel engine changes in years to come due to this convergence, and the fact that diesels emit less CO₂, a greenhouse gas of increasing concern.

Biodiesel is a notable alternative to the widely used petroleum derived diesel fuel since it can be generated by domestic natural sources such as soybeans, rapeseeds, coconuts, and even recycled cooking oil, and thus reduces dependence on diminishing petroleum fuel from foreign sources. In addition, because biodiesel is largely made from vegetable oils, it reduces lifecycle greenhouse gas emissions by as much as 78% [3,4]. There is controversy over the extent to which biodiesel and other biofuels reduce greenhouse gas emissions. Some researchers even suggest that use of biodiesel increases greenhouse gas emissions due to land use change and cultivation effects [5]. Others caution that it takes more energy input to produce than is available in the resulting biodiesel fuel output [6].

Biodiesel can be run in diesel engines without engine modification, and reduces engine emissions of HC, CO, PM relative to petroleum diesel. However, the use of biodiesel has been shown to increase NO_x by up to 20% [7]. This paper will focus on understanding the basis of the increase of NO_x when using biodiesel. We will review previously proposed theories for the NO_x increase, and then propose an additional theory.

2.0 Background

2.1. Combustion in Diesel Engines.

To help understand the process of NO_x formation in diesel engines, we will provide a short explanation of the combustion process. Diesel engines operate on the principle of compression ignition. Unlike SI engines in which a spark plug initiates combustion, diesels rely on compression in the cylinder to raise the air temperature and pressure such that upon injecting fuel, the resulting combustible mixture autoignites. The injected fuel needs to be a finely dispersed spray such that it will evaporate and mix readily with the rapidly swirling hot air in the combustion chamber. High compression

* Corresponding author. Tel: +1 510 642 9158; fax: +1 510 642 1850; *Email Address*: georgebw@me.berkeley.edu (G.A. Ban-Weiss)

ratios on the order of 12 to 24, larger than that of SI engines, are generally used in diesels to ensure high temperature and pressure, and thus autoignition of the fuel-air mixture.

The combustion process in compression ignition engines can be divided into three major sections, as shown in Figure 1 [8,9].

- (i) Ignition delay (AB): During this period the fuel spray breaks up into sub-micron droplets, and subsequently evaporates and mixes with the surrounding air. Pre-flame reactions start to occur, but ignition does not commence. The duration of the ignition delay period depends on a number of factors: how readily the fuel oxidizes, the air temperature, the size of the injected fuel droplets, and the extent of fuel-air mixing [10].
- (ii) Rapid or uncontrolled combustion (BC): In this phase, some of the mixture that has been injected into the cylinder during the ignition delay phase autoignites and starts to combust as a premixed charge. A rapid rise in pressure takes place. The rate and extent of the pressure increase depends on the amount of fuel present in the combustion chamber, which in turn depends on the length of the ignition delay.
- (iii) Controlled combustion (CD): Combustion is largely controlled by the continual rate that injected fuel mixes with the hot, compressed air in the cylinder. As the piston backs away, expansion rapidly cools the in-cylinder mixture resulting in a dramatic decrease in chemical reaction rates. Rates become so low that the term “frozen” is often applied, meaning the reaction rates are insignificant, leaving the system in a state that may be far from chemical equilibrium. High levels of NO_x and PM are examples of chemical products that are “frozen” well above their equilibrium levels.

2.2. Chemical Background of Biodiesel.

Biodiesel is oxygenated, non-toxic, biodegradable, and essentially free of sulfur and compounds with ring structures (aromatics), some of which are known to be carcinogenic. Biodiesel has a lower vapor pressure and a higher flash point than its petroleum counterpart, making it safer to handle and store [11]. Biodiesel is derived from vegetable oils or animal fats by a process known as transesterification, shown in Figure 2.

In the transesterification process, a triglyceride, which itself is an ester, is reacted with alcohol (methanol or ethanol) using a catalyst (KOH, NaOH). This process splits the triglyceride molecule into a mixture of methyl or ethyl esters of their free fatty acids (FFA) and the byproduct glycerol. Triglycerides themselves are oils composed of the glycerine ester of three fatty acids [11]. Example free fatty acids are shown in Figure 3.

Esters are named according to the alcohol used for transesterification and the FFA in the triglyceride. For example, if methanol is reacted with soybean oil, it is called a methyl ester of soybean oil. If ethanol is reacted, it is called an ethyl

ester, and so on. Further, esters differ in fatty acid chain length (medium length C15 – C18) as well as in the number of carbon double bonds. Figure 4 shows two such methyl esters. Methyl oleate has 18 carbon atoms and 1 double bond, whereas methyl linoleate has 18 carbon atoms and 2 double bonds.

Vegetable oils are triglycerides of a variety of fatty acids. Further, the relative contribution of each fatty acid attached to the glycerine can differ depending on the feedstock or the genetics of the plant used to create the triglyceride, as can be seen in Table 1. When these oil mixtures are transesterified to methyl esters, the various resulting compositions of methyl esters have been seen to lead to slightly different combustion characteristics. This mixture of methyl esters is collectively called biodiesel [11].

Using pure animal fats or raw vegetable oil (RVO) in lieu of petroleum diesel may cause severe engine deposits since the triglyceride has approximately three times the molecular mass of biodiesel and is thus more viscous and has a lower vapor pressure. A second pitfall of using RVO is the possibility of fuel congealing and hardening inside the engine and fuel lines due to its higher pour point. In addition, RVO can stick to the cylinder walls due to its low vapor pressure and be subsequently dragged into the oil pan by the piston O-rings, diluting the lubricating oil and causing higher exhaust emissions. Hence, transesterification is a way to improve the combustion characteristics and usability of raw vegetable oil by reacting the triglyceride molecule to three methyl esters, which have properties much closer to those of petroleum diesel.

Biodiesel can also be used as an additive to petroleum diesel to reduce its emissions and improve lubrication of the fuel injectors. It can be effective at concentrations as low as 1-2% [12,13]. For this reason, in 2005 the state of Minnesota began blending 2% biodiesel into nearly all diesel fuel sold throughout the state. In 2006, the U.S. Environmental Protection Agency (EPA) began requiring that all on-road diesel vehicles in the United States use Ultra Low Sulfur Diesel (ULSD), which has lubricating properties inferior to those of the previously used No. 2 diesel; this may motivate additional use of biodiesel as an additive.

2.3. NO_x Emissions of Biodiesel.

Biodiesel and biodiesel blends have been shown to have higher NO_x emissions than petroleum diesel. A review of chassis and engine tests by McCormick et al [14] gave clear evidence that a NO_x increase occurs in most cases when burning 100% biodiesel (B100) in diesel engines. However, the effect of a mixture of 20% biodiesel and 80% petroleum diesel (B20) on NO_x was less clear. On average, NO_x emissions of B20 were found to be similar to that of petroleum diesel (some studies of B20 showed higher NO_x than petroleum diesel, and some showed lower NO_x). This NO_x increase or decrease of B20 relative to petroleum diesel was found to be dependent on engine type and test cycle [14].

Since one of the aims of this investigation is to present a new explanation for the higher NO_x emissions caused by burning pure biodiesel, an overview of the most common reasons given in the literature is useful, and will now be presented. As will be seen, these explanations are closely related to effects due to premixed combustion, injection timing, soot radiation, and fuel chemistry. None of these effects should be considered to be uniquely responsible for the NO_x emissions characteristics of biodiesel; rather they should be viewed as contributing factors to NO_x emissions in various fuel and combustion situations. Finally, our new examination of this problem will be presented.

2.4. Premixed Combustion and NO_x Emissions.

As was previously mentioned, combustion inside a direct injection (DI) diesel engine starts as premixed combustion. This is a product of the fuel being injected into the combustion chamber during the initial period of ignition delay. Once autoignition commences, the accumulated fuel-air mixture that has been formed combusts as locally rich and lean pockets of premixed charge. This was labeled previously as the rapid or uncontrolled phase of combustion in this paper. The amount of charge combusted during this initial premixed phase is less than that in the controlled phase of combustion for most modern DI diesel engines. It should be noted that some small DI engines may burn a majority of their fuel in the premixed phase under certain load conditions. NO_x emissions correlate well to the amount of fuel consumed during the premixed phase of combustion, even though the flame temperature during this phase is relatively low due to the locally fuel-rich conditions [15]. With a longer ignition delay time, the reactants in the combustion chamber are increasingly preheated, which in turn increases the flame temperature and therefore causes higher NO_x emissions according to the Zeldovich mechanism (also known as thermal mechanism) [16,17]. An additional consequence of an extended ignition delay period is that more fuel is injected into the cylinder prior to autoignition and may contribute to premixed burn heat release [18]. Ignition delay time is related to a parameter called the cetane number, which will now be further discussed.

2.5. Cetane Number and NO_x Emissions.

Since premixed combustion has been theorized as a reason for the biodiesel NO_x increase, it is of interest to find a relation between cetane number and NO_x emissions. Various researchers [7,21,22] have detected a relationship between the cetane number of bio-derived fuels and their corresponding NO_x emissions. Cetane number is an indicator of the ignition delay time. Higher cetane numbers correspond to shorter ignition delay times.

Tat [21] found that biodiesel has higher cetane numbers than petroleum diesel, which would lead to a shorter ignition delay. This would lead to a non-intuitive decrease in NO_x emissions. In addition, he showed that biodiesel derived from yellow grease (waste oil collected from restaurants) had a higher cetane number and showed lower NO_x emission than

biodiesel from soybeans. McCormick et al [7] also found an inverse linear relationship between NO_x and cetane number, as shown in Figure 5. Graboski et al [23] showed that lower NO_x emissions result from more highly saturated fuels, as shown in Figure 6. Tests using cetane number enhancers such as 2-EHN or DTBN emphasized the assumption that higher cetane numbers correlate to lower NO_x emissions [22,24].

2.6. Correlation of Cetane Number to Chain Length and Degree of Saturation.

It was of interest to investigate two further correlations regarding cetane numbers for various methyl esters. An analysis of the data found in McCormick et al [7], and the Compendium of Experimental Cetane Number Data [25] led to the following two assumptions: 1) longer chains correlate with higher cetane numbers, and 2) higher degrees of saturation correlate with higher cetane numbers.

Figure 7 shows the correlation of cetane number and chain length of various methyl esters. For example, whereas methyl laurate (C12:0)[†] has a cetane number of 60, methyl stearate (C18:0) has an average cetane number of 85. Figure 7 shows that there is a linear relationship between cetane number and hydrocarbon chain length. Given the inverse linear relationship of NO_x and cetane number (Figure 5), it can be said that increasing the hydrocarbon chain length leads to reduced NO_x emissions.

Figure 8 shows that for a given chain length of 18 carbon atoms, the cetane number increases with decreasing number of double bonds, and thus higher saturation. For example, methyl linolenate, a molecule with three carbon-carbon double bonds in its hydrocarbon chain, has a cetane number of 22.7, whereas a fully saturated methyl ester of chain length 18 shows an average cetane number of 86. Combining these observations with the inverse relationship of cetane number and NO_x emissions, it can be stated that higher degrees of saturation lead to lower NO_x emissions.

[†] (C12:0) describes a molecule with a hydrocarbon chain of 12 carbon atoms and 0 double bonds

2.7. Summary of Cetane Number Effects on NO_x .

The correlation between chain length on the one hand, and double bonds on the other, explains the variation of cetane numbers and thus the variation in NO_x emissions of different biofuels. However, it does not completely explain the slight increase of NO_x for biodiesel compared to petroleum diesel. To be sure, No. 2 diesel has a cetane number of approximately 46, which is similar to that of methyl oleate (C18:1) and methyl linoleate (C18:2); however, compared to these, No. 2 diesel showed about 10% less NO_x emissions [7]. Therefore, other reasons for the slightly higher NO_x emissions besides cetane number, and thus ignition delay, need to be taken into consideration.

Remark: The Compendium of Experimental Cetane Number Data [25] shows that cetane numbers found in the literature are not as accurate as desired. Results show that measured cetane number data vary by up to 26 (e.g. for methyl stearate). Further investigations should be encouraged in this field to determine cetane numbers in a more accurate fashion.

2.8. Injection Timing and NO_x .

Injection timing is another well-studied mechanism for controlling NO_x emissions. Advancing injection timing causes higher NO_x emissions since combustion starts earlier, and thus the residence time of the burning mixture in the cylinder is increased. This allows the NO_x formation reactions to proceed. An advance in injection timing for biodiesel relative to that of petroleum diesel is caused by its higher bulk modulus of compressibility. Since pump-line-nozzle (PLN) injection systems generally start fuel injection upon reaching a certain fuel pressure, a higher bulk modulus leads to this pressure requirement being met more quickly, and thus fuel is injected earlier. Engines equipped with high-pressure common rail fuel-injection systems do not rely on the transfer of a pressure wave to initiate injection; bulk modulus is therefore not thought to alter injection timing in these types of diesel engines.

Monyem et al [26] observed a reduction in NO_x emissions of 35% to 43% for a 6-degree retardation in injection timing. An increase in the isentropic bulk modulus with degree of unsaturation was stated by Tat and Van Gerpen [27], as shown in Table 2, which correlates well with the increase in NO_x emissions for higher degrees of unsaturation.

2.9. Soot Radiation and NO_x .

Recent studies have shown that radiative heat transfer from soot can significantly influence NO_x formation in combustion systems [18,28]. It has been reported that the “cooling effect” of soot radiation may reduce NO_x emissions by approximately 25% [28]. Radiation from soot produced in the flame zone is a major source of heat transfer away from the

flame, and can lower bulk flame temperatures by 25K to 125K, depending on the amount of soot produced at the engine operating conditions. Such reductions in flame temperature would accordingly decrease the production of NO_x by the thermal mechanism by 12% to 50%. Thus, an in-cylinder soot- NO_x tradeoff exists in diesel engines. This tradeoff appears to fit biodiesel emissions data well. As stated previously, biodiesel fuels in general produce less soot than petroleum diesel fuel, which is likely a consequence of the fuel bound oxygen. This reduction in soot would in theory preclude reduction of flame temperature via radiative heat transfer, and thus leave NO_x formation unsuppressed. Also, soot radiation may explain the variation in NO_x emissions between the different esters of which biodiesel can consist. For example, methyl laurate produces 30% less soot than methyl palmitate, and thus produces 10% more NO_x [23].

2.10. Fuel Chemistry and NO_x .

Whereas the sections about premixed combustion (cetane effects), injection timing (bulk modulus effects), and soot radiation give plausible technical explanations of the variation in NO_x emissions of different biofuels and the higher NO_x emissions of biodiesel, it is useful to take a closer look at the fuel chemistry itself in order to explain the anomalous slight increase in NO_x emissions from biodiesel combustion relative to petroleum derived diesel.

As was already explained, highly saturated (no double bonds) methyl esters produce significantly lower amounts of nitrogen oxides than less saturated esters [7]. Biodiesel is a mixture of several methyl esters. Any one of these esters, if combusted individually, produces higher NO_x emissions than petroleum diesel, with the exception of the highly saturated molecules methyl palmitate (C16:0), methyl laurate (C12:0), methyl and ethyl stearate (C18:0), and the methyl and ethyl esters of hydrogenated, and thus saturated, soybean oil. This suggests that fully saturated fuels, those with no double bonds in the fatty acid chain, have the lowest NO_x emissions. Further examination of the series of laurate, palmitate, and stearate molecules also suggests that longer chain esters have lower NO_x emissions, as was previously shown in Figure 7. Therefore, McCormick et al [7] concluded that stearate fuels (C18) that have few double bonds produce significantly less NO_x than petroleum diesel.

Researchers [7] have suggested that the NO_x increase is not driven by the Zeldovich mechanism, but instead by the fact that during combustion the double bonded molecules cause higher levels of certain hydrocarbon radicals in the fuel rich zone of the diesel spray. This would result in an increased formation of Fenimore NO_x (also known as prompt NO_x). This prompted further investigation of this idea using numerical simulations as will be discussed in the next section.

3.0 Numerical Methods

As was previously discussed, biodiesel fuel tends to increase NO_x emissions relative to petroleum diesel fuel. Besides the reasons for higher NO_x emissions reviewed in the preceding sections of this paper, another explanation can be seen by the difference in molecular structure for biodiesel. As shown in Table 3, double bonded gases have higher adiabatic flame temperatures as compared to their single bonded counterparts. This temperature increase led us to postulate that the NO_x increase of biodiesel, which contains an increased amount of lower degree of saturation constituents than petroleum derived diesel, is caused by the Zeldovich mechanism. In biodiesel, anywhere from zero to three carbon-carbon pairs in the chain are connected with a double bond, which allows them only one hydrogen atom each. The remainder of this paper will provide a more in depth look at this postulation.

Further investigation of the increased NO_x formation of double bonded molecules was conducted with a numerical model for fuel-injected combustion. The simulation was carried out as a “well-mixed balloon,” the details of which are given in the next section. A complete chemical mechanism for biodiesel is not yet available because the 15 to 18 carbon chain length is too long. As this is written, mechanisms exist for a small number of molecules that contain short hydrocarbon chains, the longest of which is 8 carbons. For this reason the numerical modeling was undertaken in steps.

First, the impact of the carbon-carbon double bonds on NO_x emissions was shown in a numerical model of fuel-injected combustion for propane and propene. Propane has two single carbon-carbon bonds, and propene has one double and one single carbon-carbon bond (Figure 9). Although the molecular structure of these gases is rather simple, they are useful to determine the influence of double bonds on NO_x formation.

In the second step, methyl butanoate ($\text{nC}_3\text{H}_7\text{C}(=\text{O})\text{OCH}_3$) and its double bonded counterpart, methyl trans 2-butenate (Figure 10), were chosen. Methyl butanoate is a methyl ester analogous to those comprising biodiesel. Its chain length of three carbon atoms (C3) is significantly shorter than the usual C15-C18 found in biodiesel. However, while chain length may have an effect, we suggest that the chain length effect will be insignificant compared to the enthalpy of combustion effect, i.e. the molecule with the double bond has a higher adiabatic flame temperature.

3.1. Well-Mixed Balloon.

The “well-mixed balloon,” a variant of the “well-stirred reactor,” is a model that simulates the time history of a jet of fuel into a combustion chamber containing oxidizer. In the well-stirred reactor, the mass flow into the reactor equals the mass flow out of the reactor. In the well-mixed balloon, the mass output is zero and thus the balloon grows as mass flows in. The simulation commences as hot air entering a fuel containing balloon. In time the balloon grows and the fuel-air

mixture in the balloon reaches the ignition conditions and explodes. This leads to a sudden increase in temperature, typically higher than the temperature of the hot air entering the balloon. Further addition of the hot air now lowers the balloon temperature and drives the combustion increasingly fuel lean. The hot air mixture emulates the hot air that is entrained by a jet of fuel into a diesel engine. If the entrained air is not hot enough, the injected fuel does not ignite.

Calculations were made using Cantera, an open source chemical kinetics software similar to CHEMKIN. We ran Cantera in the MATLAB environment, although it can also be run using Python or C++. For the calculations of methyl butanoate and methyl trans 2-butenoate, a chemical mechanism file from Fisher et al [31] including thermodynamic properties for roughly 300 species and rate constants for approximately 1300 reactions was used. The complete NO_x mechanism, obtained from the GRI mechanism, was added to this mechanism file.

4.0 Results and Discussion

4.1. Propane vs. Propene.

Figure 11 shows the temperature versus time trace of the “well-mixed balloon” simulation for propane and propene at a constant pressure of 1 atm. The fuel temperature starts at 300 K, whereas the temperature of the inflowing air was 1600 K. It can be seen that the contents of the fuel jet are increasing in temperature due to the hot entrained air. Autoignition then occurs, rapidly increasing the temperature. In Figure 11, the autoignition occurs while the mixture is fuel rich. Thus, the temperature further increases as more air is entrained and the chemical reactions continue. The peak temperature occurs as the system passes through a stoichiometric fuel to air ratio. Reduction in temperature follows as the jet entrains more air. The graceful reduction in temperature (and NO_x, Figure 12) after the peak is largely due to dilution by entrained air since nearly all the chemical reactions are “frozen.” Thus peak temperatures and NO_x concentrations are used as a comparison, as shown in Table 4.

Figure 11 and Table 4 shows that propene has a higher peak flame temperature of 2782 K, as compared to 2733 K for propane. Peak NO_x emissions for propene are 13,900 ppm, 11% higher than propane NO_x emissions of 12,500 ppm, as shown in Figure 12. We explain this difference by the higher contribution of thermal NO_x due to the higher flame temperatures of propene. The earlier ignition of propene is a minor factor for higher NO_x emissions. We reduce this minor effect by using a high intake air temperature for both propane and propene (1600 K). This higher temperature brings the ignition times close together.

It should be noted that NO_x emissions comparisons between various fuels are most often performed using emissions indices, which are NO_x concentrations normalized by the concentration of emitted CO₂, a surrogate for the amount of fuel

burned. However, in these simulations the amount of each fuel compared is the same, thus the CO₂ concentrations are the same. Hence, comparison of absolute NO_x concentrations is tantamount to comparison of emission indices.

4.2. Methylbutanoate vs. Methyl trans 2-butenate.

Diesel combustion of methylbutanoate and methyl trans-2-butenate was simulated using a “well-mixed balloon” with an initial fuel temperature of 300 K, an air temperature of 1300 K, and a constant pressure of 1 atm. The NO_x and temperature vs. time traces for these two molecules are similar to that of propane and propene, which were explained in the preceding section. The peak flame temperature of methylbutanoate was found to be 2329 K, and the double bonded Methyl trans 2-butenate showed a flame temperature of 2343 K, an increase of $\Delta T = 14$ K (0.6%), as shown in Table 4. This change in temperature caused an increase in NO_x emissions of 159 ppm (21%).

4.3. Methylbutanoate Model Sensitivity Analysis.

The influence of the various NO_x mechanisms for our methylbutanoate model was investigated. The brute force method was carried out by individually removing the rate limiting equations for the mechanisms of thermal (Zeldovich), prompt (Fenimore), and N₂O NO_x. The peak NO_x emissions were calculated and Table 5 and Figure 13 shows the contribution of the different NO_x mechanisms to total NO_x. The thermal NO_x mechanism had the most visible contribution to the NO_x formation; removing the Zeldovich mechanism from the “well-mixed balloon” reduced NO_x by 92%.

A removal of the Fenimore mechanism led to a NO_x reduction of 13%. However, reducing the mechanism by both the Fenimore and the Zeldovich mechanism led to an only slightly lower reduction in NO_x than by removing the Zeldovich mechanism alone (not apparent in the table due to rounding off). As expected, the N₂O mechanism did not have an appreciable impact on NO_x formation at this point of high temperature.

4.4 Further Discussion.

When we initiated this investigation of double bond effects, we assumed that the adiabatic flame temperature consideration would be the main explanation for the slight increase in biodiesel NO_x emissions relative to petroleum diesel. We now believe that we have an additional theory to the NO_x increase, but doubt our mechanism is the sole explanation. In practice, the double bonded molecules in biodiesel will change the fuel’s physical properties such as density and bulk modulus of compressibility. The injection process (i.e. injection timing) in diesel engines with PLN type injectors is dependent on these properties; however, the injection process is generally unaffected by these properties in engines with high-pressure common rail injection systems. This suggests that the physical property differences of

biodiesel, relative to petroleum diesel, may represent a proportionally smaller contribution to the incremental NO_x increase in engines equipped with common rail injection, than those with PLN injection. Thus, since we have focused only on kinetic effects due to the double bonds, our mechanism is likely dominant in diesel engines with high-pressure common rail fuel-injection systems.

5.0 Conclusions

Numerically modeling spray combustion using a “well-mixed balloon” is an attempt toward better understanding the driving mechanisms of NO_x emissions of biodiesel. However, it is a very simplified model compared to the real process of combustion in a diesel engine [8, 10].

It was shown using our “well-mixed balloon” model that double bonded molecules have higher adiabatic flame temperatures than their single bonded counterparts. Additionally, it is well known, and has been shown in our numerical model, that even a small difference in the adiabatic flame temperature can lead to a measurable increase in NO_x emissions. Therefore, we propose an additional mechanism: the slight increase in NO_x associated with biodiesel combustion is a consequence of the degree of unsaturation of the hydrocarbon chained molecules. Unsaturated molecules tend to have higher flame temperatures and consequently the thermal (Zeldovich) NO_x mechanism is a major contributor to the incremental increase of the formation of NO_x. For a more accurate simulation, we are currently working on creating a chemical mechanism closer to that of the long carbon chain esters like methyl stearate and methyl oleate.

This work was performed under the auspices of the U. S. Department of Energy by University of California, Lawrence Livermore National Laboratory under contract W-7405-Eng-48.

References

- [1] Population and Vehicle Trends. California Air Resources Board. Online source, http://www.arb.ca.gov/app/emsinv/trends/ems_trends.php, Accessed Dec. 2006.
- [2] Kirchstetter, T.W. et al, 1999. Atmos. Environ. 33, 2955-2968.
- [3] Sheehan, J. et al, 1998. NREL Final Report. SR-580-24089.
- [4] Hill, J. et al, 2006. Proceedings of the National Academy of Sciences. 103, 30, 11206-11210.
- [5] Delucchi, M.A., 2006. Lifecycle Analysis of Biofuels. Draft Manuscript. Online source, <http://www.its.ucdavis.edu>. Accessed Dec. 2006.
- [6] Pimentel, D., Patzek, T.W., 2005. Natural Resources Research. 14, 1, 65-76.
- [7] McCormick, R. L. et al, 2003. NREL Final Report. SR-510-31465.
- [8] Stone, R., 1999. Introduction to Internal Combustion Engines, 3rd ed. SAE International, Warrendale, PA.
- [9] Owen, K., Coley, T., 1995. Automotive fuels reference book, 2nd ed. SAE International, Warrendale, PA.
- [10] Pickett, L.M. et al, 2005. SAE Technical Paper. 2005-01-3843.
- [11] Knothe, G. et al, 2005. The Biodiesel Handbook. AOCS Publishing, Urbana, IL.
- [12] Van Gerpen, J.H. et al, 1998. Evaluation of the lubricity of soybean oil-based additives in diesel fuel. Prepared for the United Soybean Board.
- [13] Munson, J.W. et al, 1999. SAE Technical Paper. 1999-01-3590.
- [14] McCormick, R.L. et al, 2006. NREL Milestone Report. MP-540-40554.
- [15] Flynn, P.F. et al, 1999. SAE Technical Paper. 1999-01-0509.

- [16] Scholl, K.W., Sorenson, S.C., 1993. SAE Technical Paper. 930934.
- [17] Choi, C.Y. et al, 1997. SAE Technical Paper. 970218.
- [18] Cheng, A.S. et al, 2006. International Journal of Engine Research. 7, 4, 297-319.
- [19] Yamane, K. et al, 2001. International Journal of Engine Research. 2, 4, 249-261.
- [20] University of Cincinnati, Department of Biology, Online source, <http://biology.clc.uc.edu/courses/bio104/lipids.htm>, Accessed January 2005.
- [21] Tat, M.E., 2003. PhD Dissertation. Iowa State University. Ames, IA.
- [22] Szybist, J. et al, 2003. SAE Technical Paper. 2003-01-3205.
- [23] Graboski, M.S. et al, 2003. NREL Final Report. SR-510-31461.
- [24] McCormick, R.L. et al, 2003. NREL Final Report. SR-510-31465.
- [25] Murphy, M.J. et al, 2004. NREL Final Report. SR-540-36805.
- [26] Monyem, A. et al, 2001. Transactions of the American Society of Agricultural Engineers. 44, 1, 35-42.
- [27] Tat, M.E., Van Gerpen, J.H., 2003. NREL Final Report. SR-510-31462.
- [28] Musculus, M., 2005. SAE Technical Paper. 2005-01-0925.
- [29] Strehlow, R.A., 1984. Combustion Fundamentals. McGraw-Hill Book Company, New York.
- [30] NIST Chemistry WebBook. Online source, <http://webbook.nist.gov/chemistry/>, Accessed January 2005.
- [31] Fisher, E.M. et al, 2000. Proceedings of the Combustion Institute. 28, 1579-1586.

Figure Captions:

- Figure 1. Hypothetical pressure versus crank angle diagram for a compression ignition engine. Modified from [8].
- Figure 2. Chemical reaction for the transesterification process. Modified from [19].
- Figure 3. Saturated and unsaturated free fatty acids. Modified from [20].
- Figure 4. Chemical structure of two FFAs: methyl oleate and methyl linoleate [19].
- Figure 5. Correlation of cetane number and NO_x emissions for various biofuels. Modified from [7].
- Figure 6. Correlation between NO_x emissions and degree of saturation. Modified from [23].
- Figure 7. Relationship between cetane number and chain length of fully saturated methyl esters. Data obtained from McCormick et al [7] and Murphy et al [25].
- Figure 8. Methyl esters cetane number vs. chain length and number of double bonds. Data obtained from McCormick et al [7] and Murphy et al [25].
- Figure 9. Molecular structure of propane (left) and propene (right).
- Figure 10. Methylbutanoate (left) and Methyl trans-2-butenoate (right).
- Figure 11. Flame temperatures of propane and propene vs. time for the numerical simulation.
- Figure 12. NO_x emissions of propane and propene vs. time for the numerical simulation.
- Figure 13. Contribution of various NO_x mechanisms to NO_x emissions of Methylbutanoate for the numerical simulation. Note that the curves for removed Zeldovich, and removed Zeldovich and Fenimore overlap.

Table Headings:

Table 1. Average Contribution of Typical Fatty Acids Contained in Plant Oils (triglycerides). Modified from [19].

Table 2. Calculated Isentropic Bulk Moduli for Various Methyl Esters. Modified from [22, 27].

Table 3. Adiabatic Flame Temperatures of Gases of the Homologous Series. Data from [29].

Table 4. Flame Temperatures and NO_x Emissions of Propane, Propene, Methylbutanoate, and Methyl trans 2-butenate from the numerical simulation.

Table 5. Influence of NO_x formation mechanisms to total NO_x in the numerical simulation.

Figure 1

[Click here to download high resolution image](#)

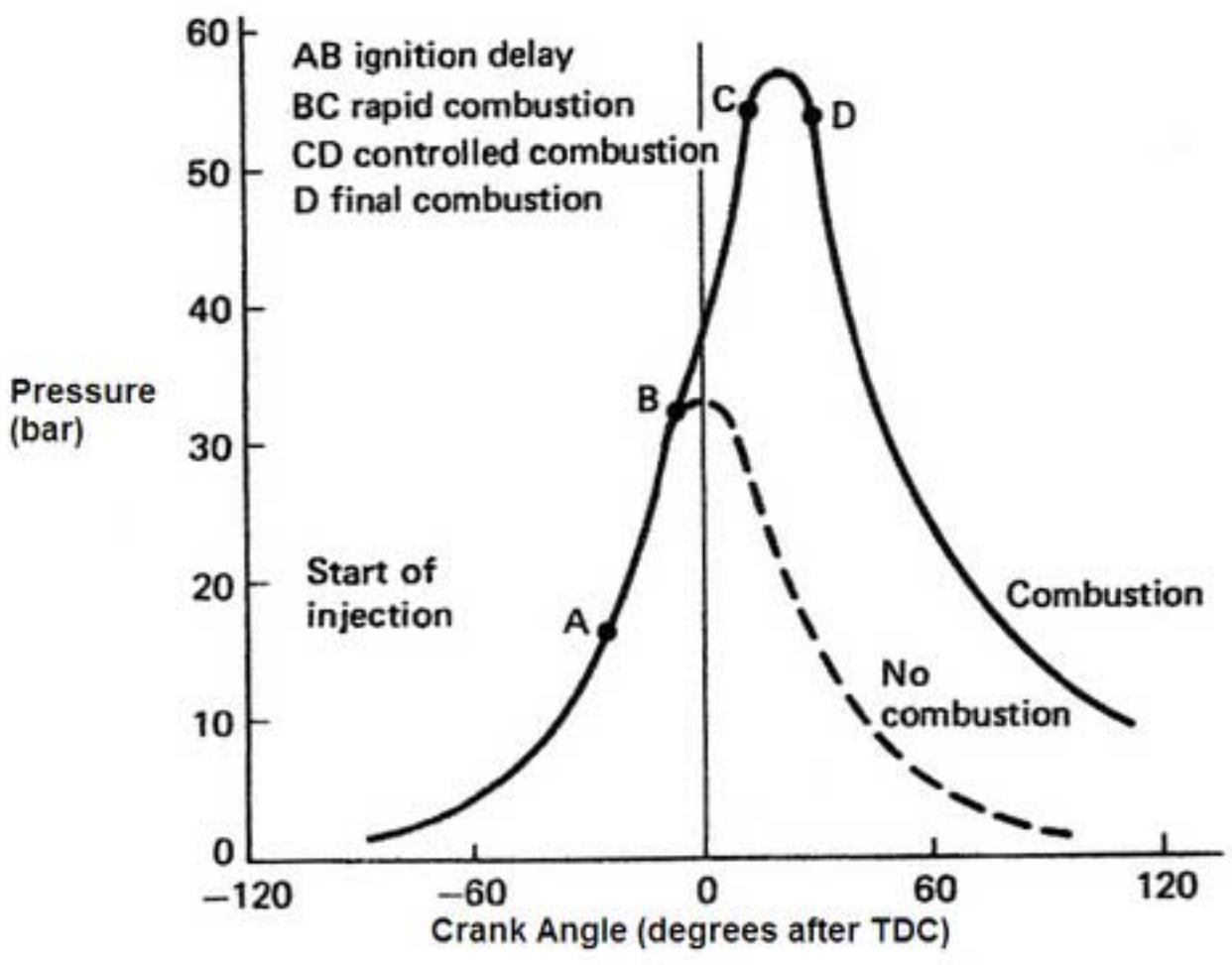


Figure 2
[Click here to download high resolution image](#)

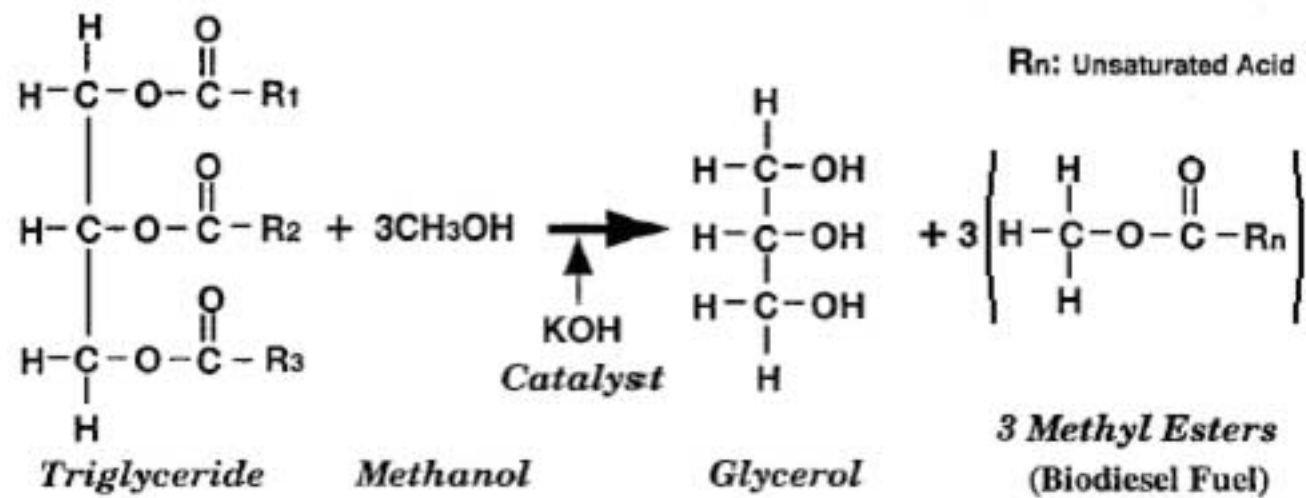
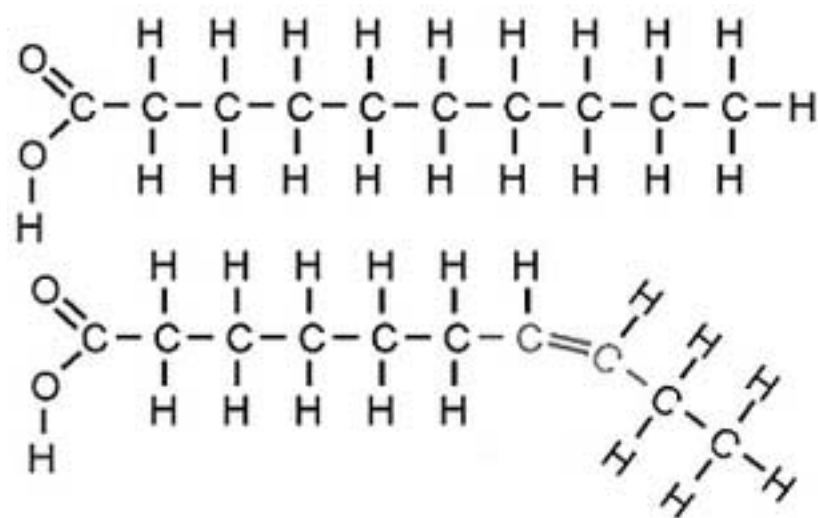


Figure 3
[Click here to download high resolution image](#)



Saturated (no C-C double bonds)

Unsaturated (contains C-C double bonds)

Figure 5
[Click here to download high resolution image](#)

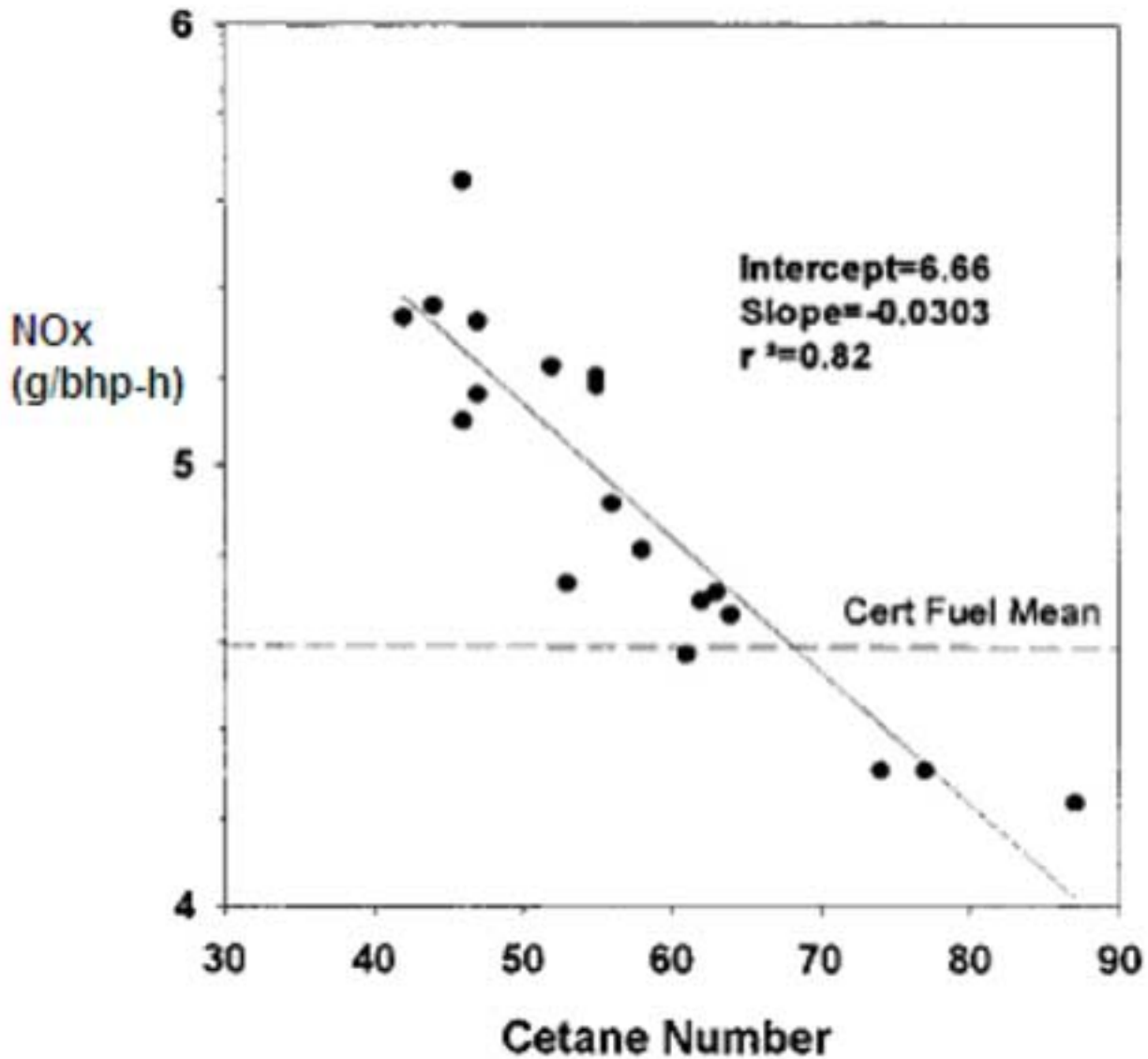


Figure 6
[Click here to download high resolution image](#)

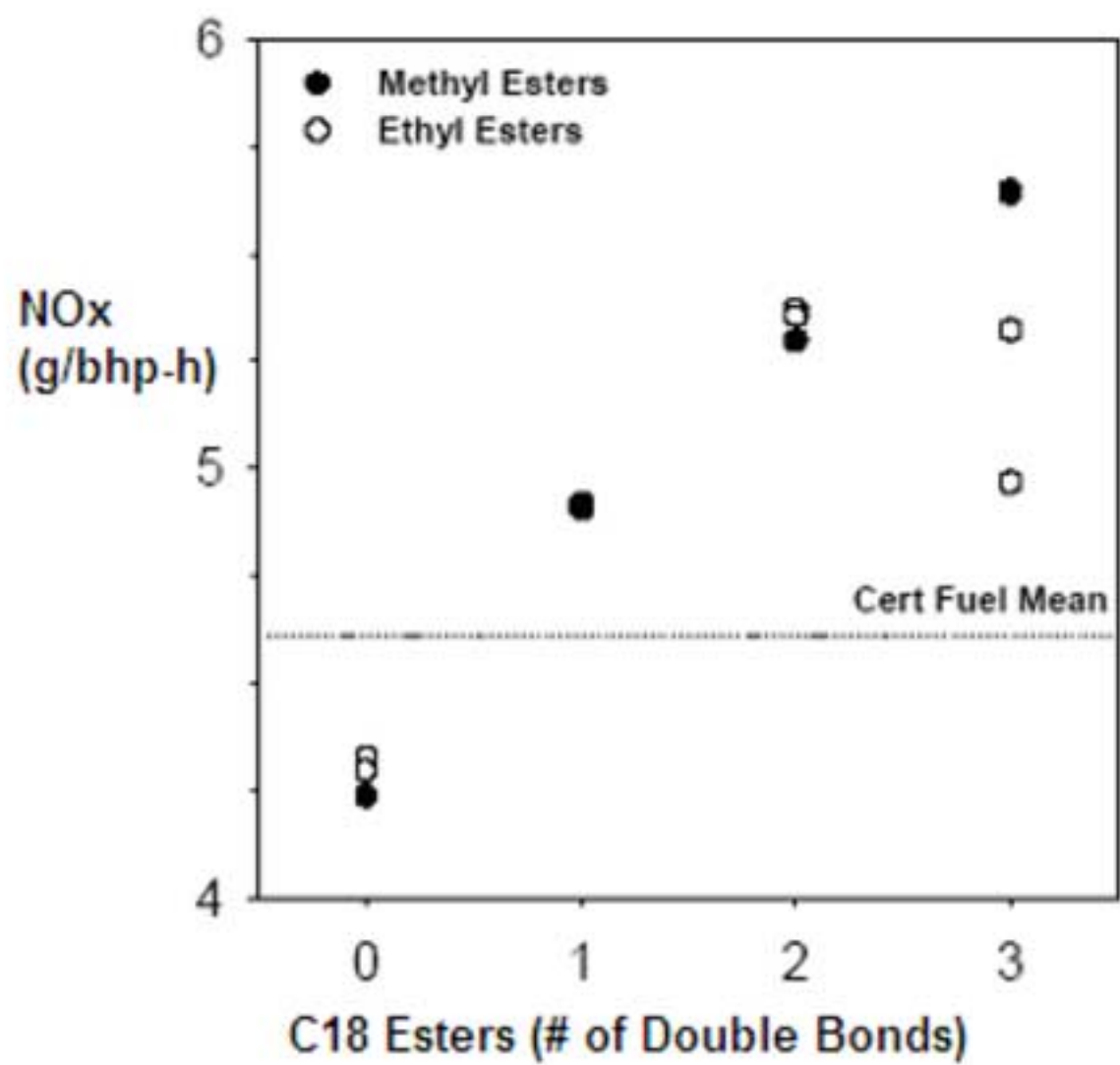


Figure 7
[Click here to download high resolution image](#)

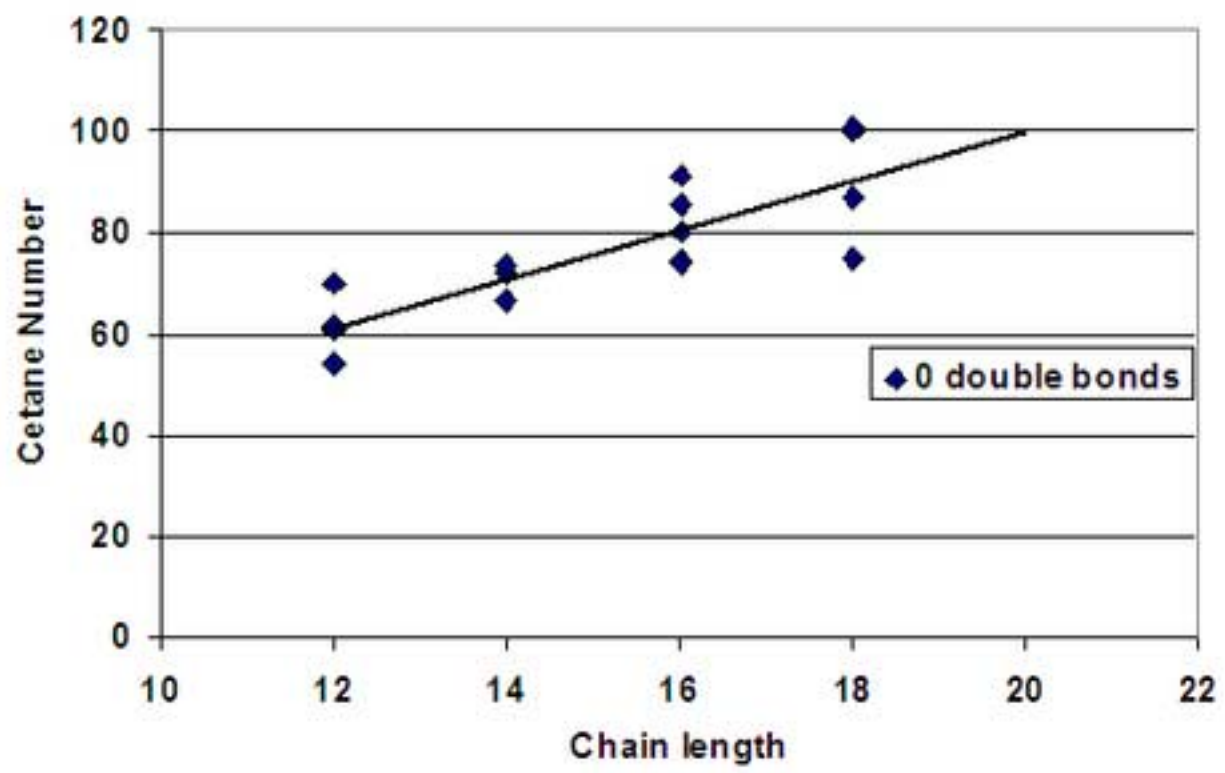


Figure 8
[Click here to download high resolution image](#)

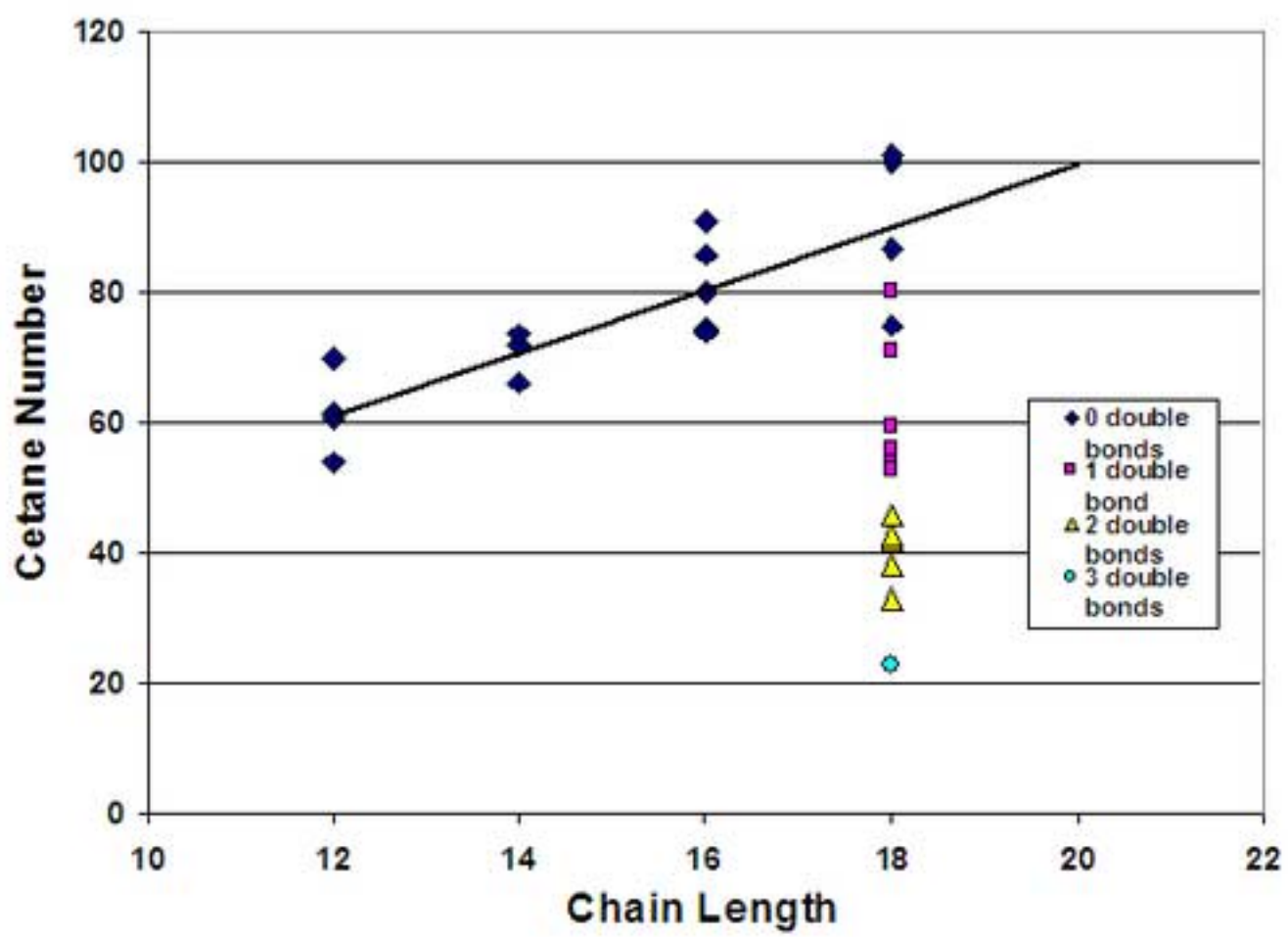


Figure 9

[Click here to download high resolution image](#)



Figure 10

[Click here to download high resolution image](#)

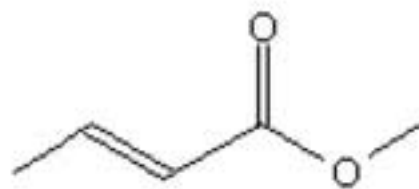
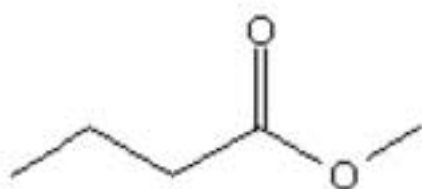


Figure 11
[Click here to download high resolution image](#)

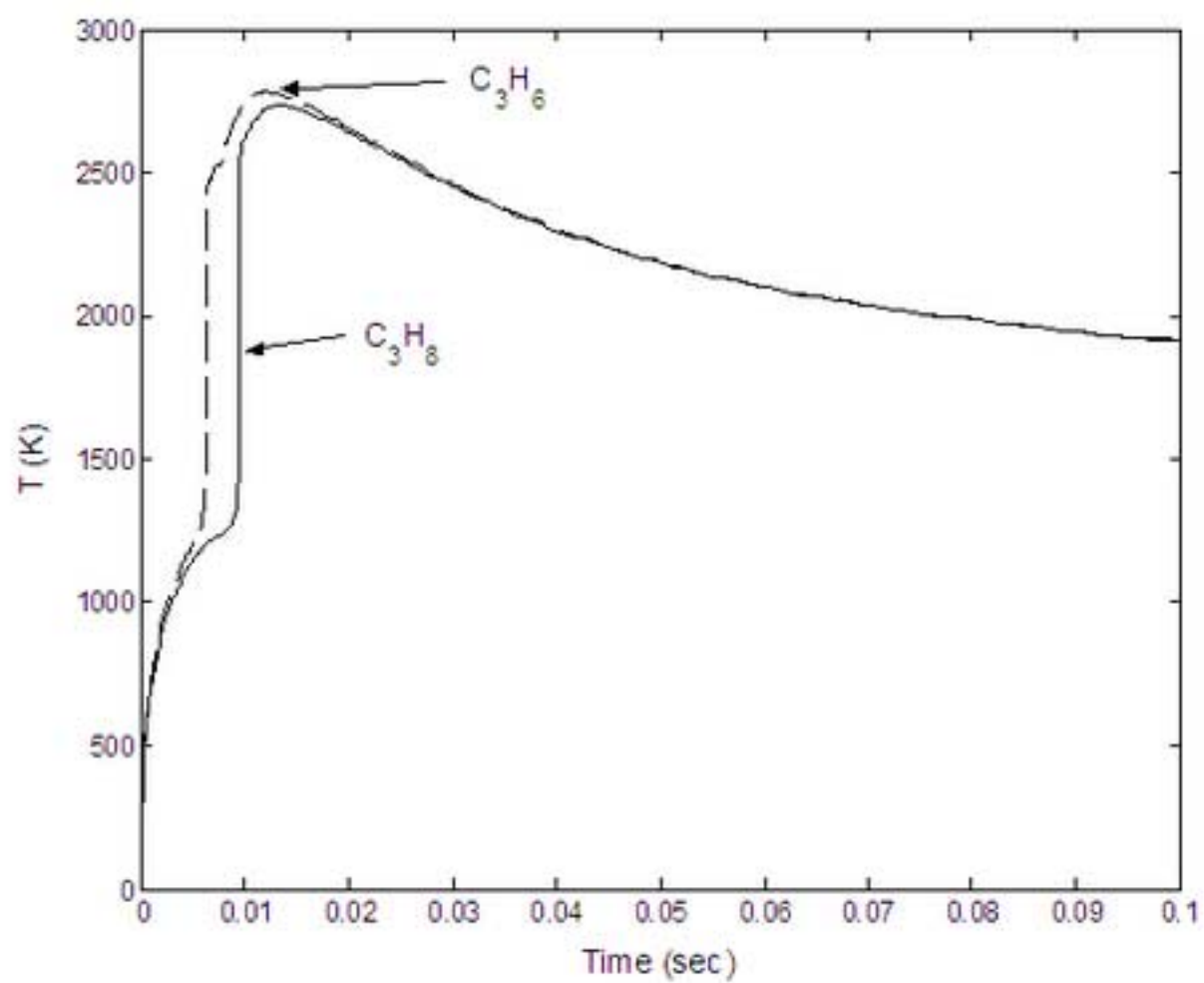


Figure 12
[Click here to download high resolution image](#)

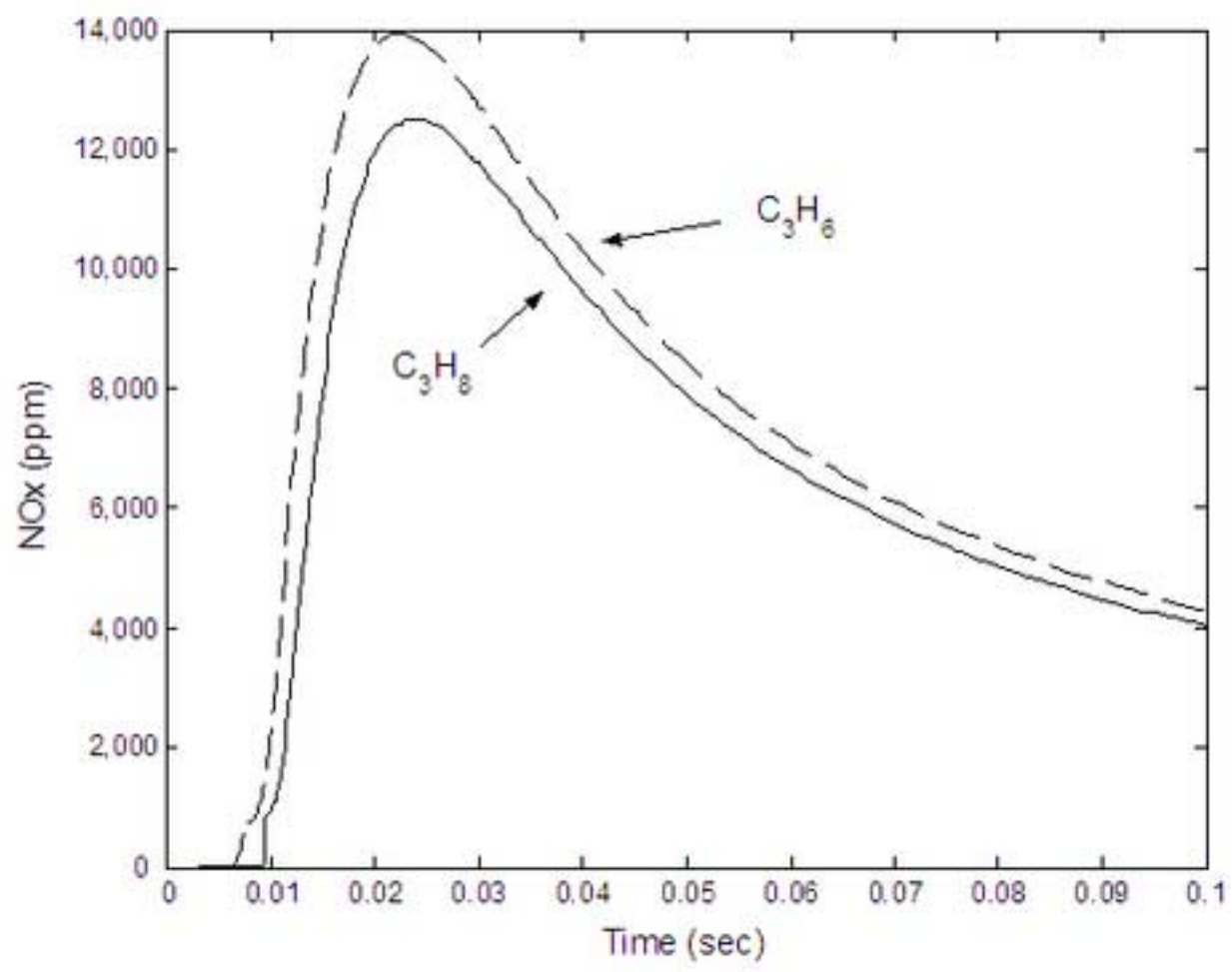


Figure 13
[Click here to download high resolution image](#)

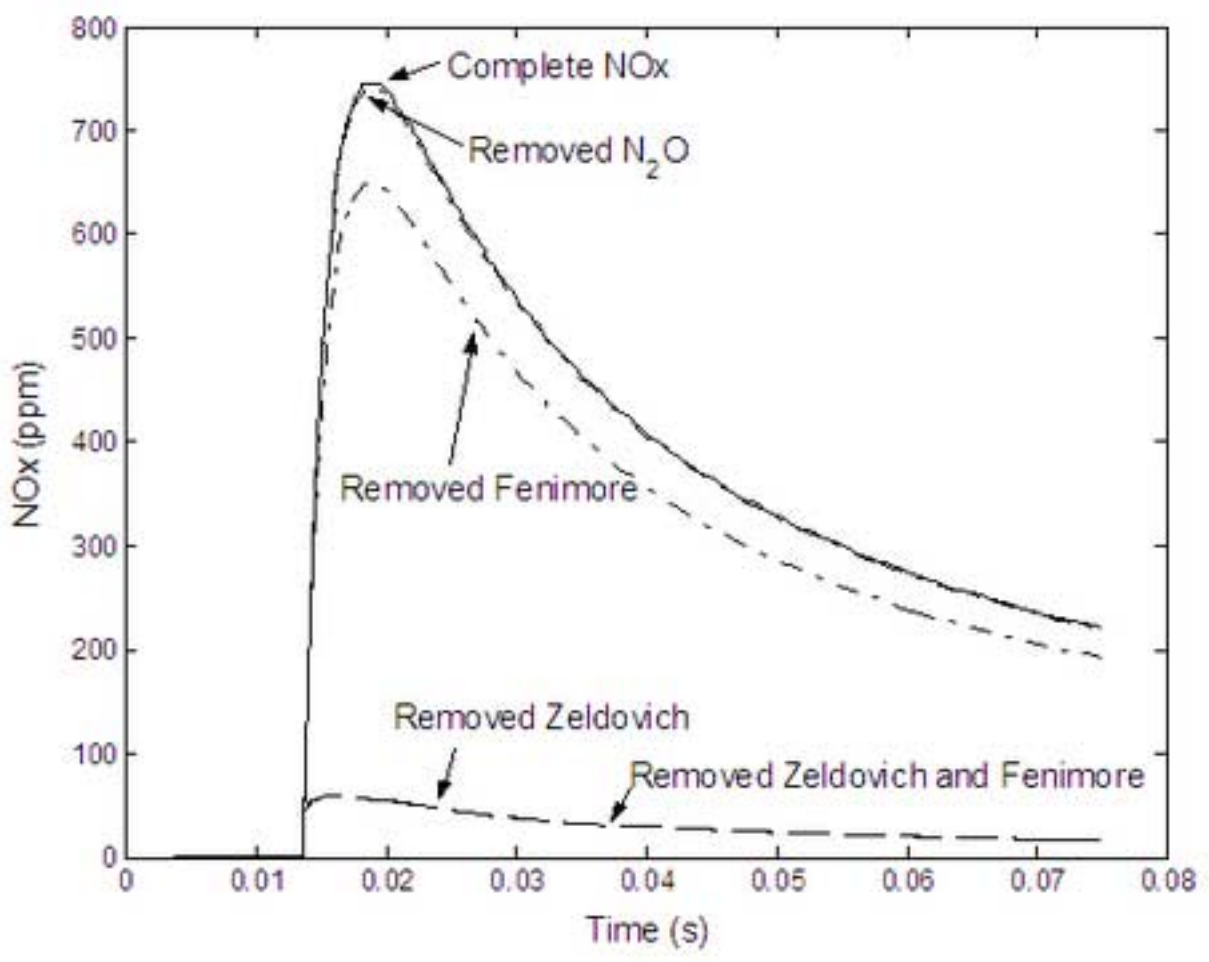


Table 1

[Click here to download high resolution image](#)

| | Rapeseed oil (vol %) | Corn oil (vol %) | Soybean oil (vol %) | Sunflower oil (vol %) |
|----------------------|-------------------------|---------------------|------------------------|--------------------------|
| Palmitic acid C16:0 | 1-4 | 7-13 | 5-12 | 3-8 |
| Stearic acid C18:0 | 0-2 | 2-5 | 2-7 | 2-5 |
| Oleic acid C18:1 | 10-35 | 25-45 | 20-35 | 15-35 |
| Linoleic acid C18:2 | 10-20 | 40-60 | 50-57 | 50-75 |
| Linolenic acid C18:3 | 1-10 | 0-3 | 3-8 | 0-1 |
| Erucic acid C22:1* | 35-60 | — | — | — |

* Not a component of cooking oil

Table 2

[Click here to download high resolution image](#)

| Ester Type: | Bulk Modulus (Mpa) |
|--------------------------|-------------------------------|
| Methyl Stearate (18:0) | 1517 |
| Methyl Oleate (18:1) | 1550 |
| Methyl Linoleate (18:2) | 1588 |
| Methyl Linolenate (18:3) | 1606 |

Table 3

[Click here to download high resolution image](#)

| Molecule | Formula | T_{adiabatic} | ΔT_{adiabatic} |
|-----------------|--------------------------------|------------------------------|-------------------------------|
| Ethane | C ₂ H ₆ | 1895 K | 80 K |
| Ethylene | C ₂ H ₄ | 1975 K | |
| Propane | C ₃ H ₈ | 1925 K | 10 K |
| Propylene | C ₃ H ₆ | 1935 K | |
| Butane | C ₄ H ₁₀ | 1835 K | 95 K |
| Butylene | C ₄ H ₈ | 1930 K | |

Table 4

[Click here to download high resolution image](#)

| | Peak temperature (K) | Peak NOx emissions (ppm) |
|---|---------------------------------|---|
| C₃H₈ | 2733 | 12500 |
| C₃H₆ | 2782 | 13900 |
| C₅H₁₀O₂ | 2329 | 747 |
| C₅H₈O₂ | 2343 | 906 |

Table 5

[Click here to download high resolution image](#)

| Removed mechanism | Peak NOx emissions (ppm) | Contribution to NOx (%) |
|----------------------------|---------------------------------|--------------------------------|
| -- | 747 | |
| N ₂ O mechanism | 742 | 1 |
| Fenimore | 650 | 13 |
| Zeldovich | 60 | 92 |
| Fenimore and Zeldovich | 59 | 92 |